

Bounding the finite-size error of quantum many-body dynamics simulations

Zhiyuan Wang,^{1,2} Michael Foss-Feig,³ and Kaden R. A. Hazzard^{1,2}

¹*Department of Physics and Astronomy, Rice University, Houston, Texas 77005, USA*

²*Rice Center for Quantum Materials, Rice University, Houston, Texas 77005, USA*

³*Honeywell | Quantum Solutions*

(Dated: September 28, 2020)

Finite-size errors, the discrepancy between an observable in a finite-size system and in the thermodynamic limit, are ubiquitous in numerical simulations of quantum many body systems. Although a rough estimate of these errors can be obtained from a sequence of finite-size results, a strict, quantitative bound on the magnitude of finite-size error is still missing. Here we derive rigorous upper bounds on the finite-size error of local observables in real time quantum dynamics simulations initiated from a product state and evolved under a general Hamiltonian in arbitrary spatial dimension. In locally interacting systems with a finite local Hilbert space, our bound implies $|\langle \hat{S}(t) \rangle_L - \langle \hat{S}(t) \rangle_\infty| \leq C(2vt/L)^{cL-\mu}$, with v the Lieb-Robinson (LR) speed and C, c, μ constants independent of L and t , which we compute explicitly. For periodic boundary conditions (PBC), the constant c is twice as large as that for open boundary conditions (OBC), suggesting that PBC have smaller finite-size error than OBC at early times. Our bounds are practically useful in determining the validity of finite-size results, as we demonstrate in simulations of the one-dimensional quantum Ising and Fermi-Hubbard models.

Introduction Numerical simulations are crucial to our understanding of many-body quantum matter, and are routinely applied in all fields of physics and in chemistry. Numerical calculations are used to understand equilibrium properties of strongly correlated quantum materials [1–9], model nonequilibrium dynamics of ultracold matter [10–18], calculate molecular properties [19–21], and determine nuclear structure [22–26], as a few examples.

Unfortunately, many numerical techniques popular in these fields incur significant finite-size errors when approximating properties of a large (potentially infinite) system by properties of a finite one. The most direct example is exact diagonalization (ED), which exactly solves the finite system numerically [8, 27–29]. Accessible system sizes are limited since the Hilbert space dimension grows exponentially with system size; for the simplest case of interacting spin-1/2s, a state-of-the-art ground state calculation is limited to ~ 45 spins [30]. Finite-size errors also significantly affect other techniques, such as density matrix renormalization group (DMRG) [31–34], many tensor network algorithms [35], and quantum Monte Carlo (QMC) [36], and they are a significant source of error for simulating quantum systems on quantum computers (Ref. [37] overviews some of these methods) and for analog quantum simulations using ultracold matter [38], trapped ions [39], and other platforms [40].

It is often difficult to characterize finite-size errors. The standard method to assess them is to calculate observables for different system sizes and check how much the results differ, ideally employing finite-size scaling. Although useful, this method has severe limitations. One is that it offers no guarantees. Two different system sizes may have results in close agreement, but at larger sizes the physics changes and observables deviate [41]. An-

other is that one may not be able to study multiple system sizes that are sufficiently large to get a good estimate of the convergence.

In this paper, we consider non-equilibrium dynamics initiated from product states and derive *rigorous* upper bounds on the error of approximating observables in a large, possibly infinite, quantum many-body system by results in a smaller one. The bounds are applicable to arbitrary Hamiltonians provided that a LR bound exists. In locally interacting systems with a finite local Hilbert space, the bound for a local observable \hat{S} is given by

$$|\langle \hat{S}(t) \rangle_L - \langle \hat{S}(t) \rangle_\infty| \leq C(2vt/L)^{cL-\mu}, \quad (1)$$

where v is the LR speed, and $C, c,$ and μ are constants that depend on the Hamiltonian, observable, and boundary condition. (A tighter form that is still efficiently computable, but less analytically simple, is also given below.) Such dynamics is explored in a wide variety of ultracold matter experiments. Representative examples are experiments that have studied quantum quenches in Rydberg atoms [42–47], molecules [48–50], Fermi gases [51], atoms in optical lattices [52–56], and optical clocks [57]; and which have explored slow ramps in Rydberg atoms [45, 46]. This dynamics can probe fundamental physical phenomena, such as many-body localization [58–62], prethermalization [63, 64], and generation of topological defects near critical points [65].

The idea behind our bound is that locality – specifically that one piece of a system does not instantly affect far-away pieces – imposes strong constraints on quantum dynamics [66, 67]. This can be seen by considering evolution under a Hamiltonian initiated from a product state. As illustrated in Fig. 1, an observable in a region X will be affected by finite-size errors only after a long enough time for information to propagate from the boundary to

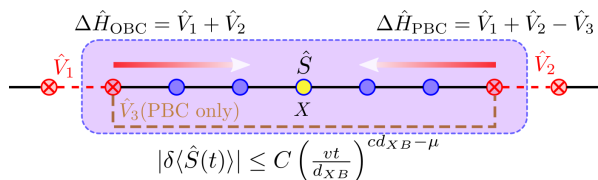


FIG. 1. Finite-size simulation of a 1D system. In locally interacting systems, information propagates no faster than the LR speed v , so it takes a finite amount of time $t_c \sim d_{XB}/v$ for the boundary interaction $\Delta \hat{H}$ to affect the center site observable \hat{S} . Here d_{XB} is the minimal distance between the support X of the observable $\hat{S}(t)$ (yellow circle in the center) and the support B of $\Delta \hat{H}$ (red crossed boundary sites near the dashed links).

X . This idea is made precise by relating finite-size error to unequal time correlation functions, which can then be bounded by a LR bound [68], a direct consequence of locality. Although similar ideas of applying LR bounds to analyze the performance of some numerical algorithms have been employed in Refs. [69–76], the connection to finite-size error has not been made explicit, and the practical utility of the bounds for numerics was not demonstrated.

Our finite-size error bound not only shows the convergence of finite-size approximations in principle, but is tight enough to be useful in practice, which we demonstrate in simulations of some prototypical models. For example, in the dynamics following a sudden change of parameters in a one-dimensional transverse field Ising model (TFIM) with $L = 21$ sites, the error bounds for the transverse magnetization and nearest-neighbor correlations remain extremely small to times where they have evolved close to equilibrium. Furthermore, the bounds are reasonably tight: the time at which the error bound becomes significant is 20–25% smaller than the time at which the actual finite-size error becomes noticeable. We similarly demonstrate this for the non-equilibrium dynamics of the Fermi-Hubbard model (FHM) relaxation from a checkerboard state, inspired by experiments and theory of Refs. [12, 16]. The precision of these bounds is enabled by the major quantitative improvements offered by recent LR bounds [77, 78].

In addition to their quantitative utility, these bounds provide several insights into the convergence of numerical methods, and open the way to designing new algorithms. One immediate consequence of the bounds is to rigorously show that the finite-size error decays exponentially with the linear dimension of the system for periodic boundary condition (PBC), as well as for open boundary condition (OBC) provided that one measures observables only near the center of the system, as commonly employed in the DMRG community. If one instead averages the measurement over all sites in OBC, then our bound indicates that the error decays only algebraically. Simi-

lar behavior at finite temperature has been observed and analyzed in Ref. [79]. Furthermore, if one compares PBC to OBC with center site measurement, our error bound for PBC decays twice as fast with distance as the bound for OBC at early times, suggesting that PBC gives more reliable results at early times [80]. These insights may lead to new methods; one example is that they show why the moving-average cluster expansion (MACE) method of Ref. [49] converges exponentially faster than alternative schemes.

A simple bound for both OBC and PBC Consider the dynamical evolution of a quantum many-body system on an infinite d -dimensional lattice, governed by a locally interacting Hamiltonian \hat{H} . For illustrative purpose, in Fig. 1 we draw the configuration for a 1D nearest-neighbor interacting lattice model. Let $|\psi\rangle$ be the initial product state, \hat{S} be a local observable to be measured that acts on a finite region X (center point in Fig. 1), and let $\Delta \hat{H} = \sum_j \hat{V}_j$ be the sum of all the interaction terms between the inner and outer parts of the system (red links in Fig. 1). If PBC are used, we further subtract from $\Delta \hat{H}$ the interaction between the first and the last site (brown link in Fig. 1). Let \hat{H}_L and $|\psi_L\rangle$ denote the Hamiltonian and the initial state of the finite-size simulation, respectively (i.e. the restriction of \hat{H} and $|\psi\rangle$ to the L -site inner system). Denote $\hat{H}' = \hat{H} - \Delta \hat{H}$, so that \hat{H}' decouples into two commuting terms, one acting only on the inner system, the other acting only on the outer system. The finite-size error of the observable \hat{S} is

$$\delta \langle \hat{S}(t) \rangle_\psi \equiv |\langle e^{i\hat{H}_L t} \hat{S} e^{-i\hat{H}_L t} \rangle_{\psi_L} - \langle e^{i\hat{H} t} \hat{S} e^{-i\hat{H} t} \rangle_\psi|. \quad (2)$$

where $\langle A \rangle_\psi \equiv \langle \psi | A | \psi \rangle$, and we set $\hbar = 1$ throughout. Since \hat{H}' decouples into two independent spatial regions (inner and outer) and $|\psi\rangle$ is a product state, the first term in Eq. (2) can be rewritten as $\langle e^{i\hat{H}' t} \hat{S} e^{-i\hat{H}' t} \rangle_\psi$. Inserted into Eq. (2), the two expectation values are taken in the same state $|\psi\rangle$, so their difference can be bounded by the operator norm $|\langle \psi | \hat{A} | \psi \rangle| \leq \|\hat{A}\|$. Using the unitary invariance of operator norm $\|\hat{A}\| = \|\hat{U} \hat{A} \hat{V}\|$ for arbitrary unitary operators \hat{U}, \hat{V} , we have

$$|\delta \langle \hat{S}(t) \rangle_\psi| \leq \|\hat{U}_I(t) \hat{S} \hat{U}_I(t)^\dagger - \hat{S}\|. \quad (3)$$

where $\hat{U}_I(t) = e^{-i\hat{H} t} e^{i\hat{H}' t}$ is the evolution operator in the interaction picture, which satisfies $\hat{U}_I(0) = 1$ and $i\partial_t \hat{U}_I(t) = \hat{U}_I(t) \Delta \hat{H}(t)$, where $\Delta \hat{H}(t) = e^{-i\hat{H}' t} \Delta \hat{H} e^{i\hat{H}' t}$. Now applying the fundamental theorem of calculus and the triangle inequality, we obtain a bound on the finite-size error given by

$$\begin{aligned} |\delta \langle \hat{S}(t) \rangle_\psi| &\leq \int_0^t \left\| \frac{d}{dt'} [\hat{U}_I(t') \hat{S} \hat{U}_I(t')^\dagger - \hat{S}] \right\| dt' \\ &= \int_0^t \|\hat{U}_I(t') [\Delta \hat{H}(t'), \hat{S}] \hat{U}_I(t')^\dagger\| dt' \\ &= \int_0^t \|\Delta \hat{H}(t'), \hat{S}\| dt'. \end{aligned} \quad (4)$$

The integrand is the quantity bounded by LR bounds, so to upper bound the finite-size error, one can insert the relevant LR bound. We focus on locally interacting systems, but Eq. (4) applies equally to long-range interactions by substituting the corresponding LR bounds [76, 81–90] in those systems. For a locally-interacting system, the currently tightest LR bound is obtained by computing the series in Eq. (S10) of the Supplemental Material [91], which is based on Refs. [77, 78], although this may not be efficiently computable in general. A slightly looser but efficiently computable method is discussed in Ref. [78], in which one solves a system of first order linear differential equations for a number of variables proportional to the system size. To see the qualitative features of the bound for large systems, we can insert the simple expression given in Eq. (3) of Ref. [78] into Eq. (4) to obtain

$$|\delta\langle\hat{S}(t)\rangle_\psi| \leq \sum_j c_j \left(\frac{v|t|}{d_{Xj}}\right)^{D(\hat{S}, \hat{V}_j)}, \quad (5)$$

where c_j are constants independent of t and d_{Xj} , $D(\hat{S}, \hat{V}_j)$ is the distance between the operators \hat{S}, \hat{V}_j in the commutativity graph (CG) as introduced in Ref. [78], and u is the LR speed in CG. The distance in the CG is related to the distance in real space d_{Xj} by $D(\hat{S}, \hat{V}_j) = \eta d_{Xj} - \mu$, where η, μ are (straightforwardly determined) constants, and d_{Xj} is the distance between X and j in real space. Therefore the rhs of Eq. (5) can be bounded by $(\frac{vt}{d_{XB}})^{\eta d_{XB} - \mu}$, where $d_{XB} = \min_{j \in B} d_{Xj}$. Despite its simplicity, the t -dependence of this bound generically agrees with that of the exact error to lowest order in t in OBC [91].

Besides its practical utility for bounding finite-size error in calculations, as demonstrated below, this result has qualitative implications. One is to rigorously support the common practice of measuring observables close to the center site in OBC numerics (e.g. in the DMRG community), rather than averaging over all sites. This minimizes the error bound, since the center size maximizes d_{XB} . This choice yields our main result in Eq. (1) for the OBC case. Our bound allows one to extend this. For example, in dimension greater than one, we can minimize finite-size error by choosing an optimal cluster shape that minimizes the rhs of Eq. (5), and run simulations on the optimal shape.

An improved bound for PBC In the previous section we treated PBC in a way similar to OBC. But it turns out that the resulting bound in Eqs. (4) and (5) is qualitatively loose at small t for PBC. The reason for this can be intuitively understood as follows. The two terms in the rhs of Eq. (2) can be expanded in t . As we discuss in greater detail in the Supplemental Material [91], the finite-size error for $\hat{S}(t)$ actually is only contributed by terms in $e^{i\hat{H}t}\hat{S}e^{-i\hat{H}t}$ whose spatial span is larger than L and terms in $e^{i\hat{H}Lt}\hat{S}e^{-i\hat{H}Lt}$ that wrap around the whole

periodic system. The leading order of these terms is proportional to $t^\mathcal{L}$, where \mathcal{L} is the length of the shortest non-contractible loop on the PBC commutativity graph, which is roughly twice as large as the exponent $D(\hat{S}, \hat{V}_j)$ in Eq. (5). The Supplemental Material [91] extends methods developed in Refs. [77, 78] to derive a rigorous upper bound for $|\delta\langle\hat{S}(t)\rangle|$ that leads to this improved $t^\mathcal{L}$ scaling. For simplicity, let us focus on 1D nearest-neighbor interacting Hamiltonians $\hat{H} = \sum_j \hat{h}_j$ (where \hat{h}_j acts on sites $j, j+1$), and consider an observable \hat{S} acting on a single site i . The analog of Eq. (4) is

$$|\delta\langle\hat{S}(t)\rangle| \leq 2 \sum_{|j-i| \leq L} \int_0^t dt' \|\hat{h}_j, \hat{S}_j^L(t') - \hat{S}_j^{L-1}(t')\|, \quad (6)$$

where $\hat{S}_j^L(t) \equiv e^{i\hat{H}_j^L t} \hat{S} e^{-i\hat{H}_j^L t}$, \hat{H}_j^L is the truncation of \hat{H} that acts on the L consecutive sites containing i and exactly one of $j, j+1$, and similarly for $\hat{S}_j^{L-1}(t)$. Eq. (6) can be straightforwardly generalized to higher dimension and arbitrary locally interacting Hamiltonians. In the Supplemental Material [91] we give three different methods to obtain improved LR bounds for the integrand in Eq. (6). The analytically simplest one is

$$|\delta\langle\hat{S}(t)\rangle_\psi^{(\text{PBC})}| \leq \sum_{1 \leq p \leq d} C_p \left(\frac{2v_p t}{L_p}\right)^{\mathcal{L}_p}, \quad (7)$$

where the constant C_p is given in Eq. (S43), v_p is the LR speed in the p -th direction given in Eq. (S44), and \mathcal{L}_p is the size of the periodic system in the p -th direction in commutativity graph. \mathcal{L}_p is related to the real space system size L_p by $\mathcal{L}_p = \eta_p L_p - \mu_p$ for constant integers η_p, μ_p . The other two methods do not always give a simple analytic expression, but are tighter than Eq. (7). In the numerical examples below, we use the tightest one, which is based on the method in Ref. [77]. We note that while all of these improve the small-time exponent of the PBC bound by a factor of 2 compared to Eqs. (4) and (5), the timescale $t_c \approx \min_p L_p / 2v_p$ on which the bound exponentially grows is still approximately the same as Eq. (5). Besides its quantitative utility, Eq. (7) shows that in anisotropic systems where v_p is different in each direction, one should choose $L_p \propto v_p$ in order to minimize the finite-size error.

Example: 1D TFIM We test our error bounds in numerical simulations of prototypical models for quantum many-body physics, starting with the TFIM,

$$\hat{H} = -J \sum_j \hat{\sigma}_j^z \hat{\sigma}_{j+1}^z - h \sum_j \hat{\sigma}_j^x. \quad (8)$$

This is a canonical model in which to study quantum phase transitions [92, 93], and has been realized in materials like CoNb_2O_6 [94] and cold atom [95–97] and trapped ion [98–102] experiments, and simulated in superconducting circuits [103, 104]. We numerically study

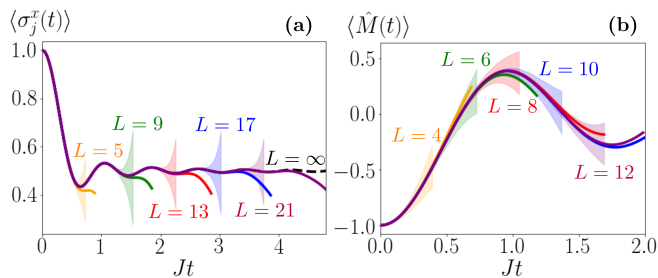


FIG. 2. Numerically exact evolution for (a) $\langle \hat{\sigma}_j^x(t) \rangle$ in the L -site PBC TFIM at $J = h$, from the initial state $|\rightarrow \rightarrow \dots \rightarrow\rangle$, and (b) $\langle \hat{M}(t) \rangle$ in the L -site OBC FHM at $U = 0.5J$, from the initial state $|202020\dots 20\rangle$. The dashed curve in TFIM is the exact $L \rightarrow \infty$ result. The shaded areas for each curve represent the region in which the true thermodynamic limit result must lie according to the finite-size error bounds in Eqs. (9) and (4), respectively.

the quantum dynamics of this model at the critical point $J = h$ for several system sizes, and calculate the exact evolution in the thermodynamic limit. Specifically, we study the dynamics of $\langle \hat{\sigma}^x(t) \rangle$ starting from the state $|\psi(0)\rangle = |\rightarrow \rightarrow \dots \rightarrow\rangle$. Analogous dynamics in the 2D TFIM has been explored in experiment with Rydberg atoms [45, 46].

Fig. 2a shows $\langle \hat{\sigma}_j^x(t) \rangle$ in different system sizes from $L = 5$ to $L = 21$, using PBC. As a comparison, we also plot the exact solution in the thermodynamic limit given in Ref. [105]. To obtain a rigorous finite-size error bound for $\langle \hat{\sigma}_j^x(t) \rangle$, we use the LR bound given in Eq. (S15) of the Supplemental Material [91] [which is an application of the general bound Eq. (S11)], which, after inserting into Eq. (4), yields

$$|\delta \langle \hat{\sigma}_j^x(t) \rangle| \leq 4\sqrt{\frac{J}{h}} \frac{(2\sqrt{Jht})^{2L-1}}{(2L-1)!} + \frac{J}{h} \frac{(4\sqrt{Jht})^{2L-2}}{(2L-2)!}. \quad (9)$$

As Fig. 2a shows, this rigorous error bound provides a useful guarantee of the numerical calculations' accuracy out to interesting and useful timescales. For the $L = 21$ -site calculation, the bounds guarantee that the results are extremely accurate (within 10^{-2}) up to times $Jt \sim 3.5$, where the observable has already come close to equilibration. Furthermore, this time to which the bounds remain useful is in reasonable accord with the true time at which finite size error becomes important (within 20%).

We emphasize that the derivation of the error bound never made use of the exact solution of the TFIM. The bound Eq. (4) can be applied to any system including in dimensions greater than one. As we demonstrate in the 1D FHM, the bound still provides a useful, rigorous guarantee of the finite-size simulation results when no exact solution is available.

Example: The FHM The 1D FHM describes spin-1/2 fermions in a lattice whose Hamiltonian is

$$\hat{H} = -J \sum_{\langle ij \rangle, \sigma = \uparrow, \downarrow} (\hat{a}_{i\sigma}^\dagger \hat{a}_{j\sigma} + \text{H.c.}) + U \sum_i \hat{n}_i^\uparrow \hat{n}_i^\downarrow. \quad (10)$$

The model exhibits rich behavior, such as a metal-Mott insulator transition, and in higher dimension it may display phenomena associated with high-temperature superconductors. It is a reasonable approximation of a number of materials such as transition-metal monoxides (FeO, NiO, CoO) [106], and has been realized in ultracold atoms [107–111].

We numerically study the relaxation dynamics of a charge density wave state $|\psi(0)\rangle = |202020\dots 20\rangle$, analogous to calculations in Ref. [17] and experiments in Ref. [112], where 2 means a doubly occupied site, $a_{j\uparrow}^\dagger a_{j\downarrow}^\dagger |\text{vac}\rangle$, while 0 means an empty site. We run the finite-size simulations in OBC for system sizes from $L = 4$ to $L = 12$, and measure the density imbalance $\hat{M}(t)$ defined as $\hat{M}(t) = [\hat{N}_{\text{even}}(t) - \hat{N}_{\text{odd}}(t)]/L$ [17]. To get a rigorous finite-size error bound for $\hat{M}(t)$, we use the currently tightest LR bound, given in Eq. (S10) of the Supplemental Material [91] [numerically summing the series on the commutativity graph of the FHM shown in Fig. S2] and insert into Eq. (4). The simulation results are shown in Fig. 2b.

Our error bound can be compared to estimates of finite-size error obtained from comparing calculations of different sizes. For example, one can take the difference between the $L = 10$ and $L = 12$ as a rough estimate of the finite-size error of the $L = 12$ calculation. Our bound is comparable in its guaranteed timescale of convergence to this conventional estimate. For example, we can guarantee that the finite size error in $\langle \hat{M}(t) \rangle$ of the $L = 12$ result is less than 1% for $Jt \leq 1.2$, comparable to the time $Jt \sim 1.6$ where the $L = 10$ and 12 results differ noticeably.

Conclusions We have presented a rigorous upper bound on the finite size error of local observables measured in numerical simulations of quantum dynamics, for arbitrary Hamiltonians in arbitrary dimensions. Specifically, we derived a simple bound that works for both OBC and PBC, and an improved bound for PBC. These are often qualitatively tight at early times. To apply these bounds in specific models, one inserts the corresponding LR bounds into the rhs of Eq. (4) or Eq. (6). The bounds rigorously show that the finite-size errors decay super-exponentially $\delta \langle \hat{S}(t) \rangle \propto e^{-L \ln L}$ in system size, and guarantee the accuracy of finite size simulation below a time scale $t_c \sim L/2v$.

The quantitative utility of the bounds is demonstrated in the 1D TFIM and 1D FHM. In both cases, the bounds give rigorous, quantitatively useful results to timescales where there is interesting physics and even equilibration. They are reasonably tight: they indicate the time at which the finite size errors become appreciable within

about 30%. The bounds provide new insights into finite size errors, and can motivate better algorithms.

We thank Miles Stoudenmire, Miroslav Hopjan, Bhuvanesh Sundar and Ian White for discussions, and Brian Neyenhuis for a careful reading of the manuscript. This work was supported in part by the Welch Foundation (C-1872), the National Science Foundation (PHY-1848304), and the Office of Naval Research (N00014-20-1-2695).

-
- [1] J. E. Hirsch, Phys. Rev. B **31**, 4403 (1985).
- [2] S. R. White, D. J. Scalapino, R. L. Sugar, E. Loh, J. E. Gubernatis, and R. T. Scalettar, Phys. Rev. B **40**, 506 (1989).
- [3] A. W. Sandvik and J. Kurkijärvi, Phys. Rev. B **43**, 5950 (1991).
- [4] S. R. White and D. A. Huse, Phys. Rev. B **48**, 3844 (1993).
- [5] M. Caffarel and W. Krauth, Phys. Rev. Lett. **72**, 1545 (1994).
- [6] W. M. C. Foulkes, L. Mitas, R. J. Needs, and G. Rajagopal, Rev. Mod. Phys. **73**, 33 (2001).
- [7] S. Yan, D. A. Huse, and S. R. White, Science **332**, 1173 (2011).
- [8] A. W. Sandvik, AIP Conf. Proc. **1297**, 135 (2010).
- [9] E. M. Stoudenmire, J. Alicea, O. A. Starykh, and M. P. A. Fisher, Phys. Rev. B **84**, 014503 (2011).
- [10] S. R. White and A. E. Feiguin, Phys. Rev. Lett. **93**, 076401 (2004).
- [11] A. N. Rubtsov, V. V. Savkin, and A. I. Lichtenstein, Phys. Rev. B **72**, 035122 (2005).
- [12] S. Trotzky, Y.-A. Chen, A. Flesch, I. P. McCulloch, U. Schollwöck, J. Eisert, and I. Bloch, Nat. Phys. **8**, 325 (2012).
- [13] J. P. Ronzheimer, M. Schreiber, S. Braun, S. S. Hodgman, S. Langer, I. P. McCulloch, F. Heidrich-Meisner, I. Bloch, and U. Schneider, Phys. Rev. Lett. **110**, 205301 (2013).
- [14] N. Y. Yao, C. R. Laumann, S. Gopalakrishnan, M. Knap, M. Mueller, E. A. Demler, and M. D. Lukin, Phys. Rev. Lett. **113**, 243002 (2014).
- [15] C. Karrasch, J. Moore, and F. Heidrich-Meisner, Phys. Rev. B **89**, 075139 (2014).
- [16] A. Bauer, F. Dorfner, and F. Heidrich-Meisner, Phys. Rev. A **91**, 053628 (2015).
- [17] N. Schlünzen, J.-P. Joost, F. Heidrich-Meisner, and M. Bonitz, Phys. Rev. B **95**, 165139 (2017).
- [18] P. Bordia, H. Lüschen, U. Schneider, M. Knap, and I. Bloch, Nat. Phys. **13**, 460 (2017).
- [19] P. J. Reynolds, D. M. Ceperley, B. J. Alder, and W. A. Lester Jr, J. Chem. Phys. **77**, 5593 (1982).
- [20] P. W. Atkins and R. S. Friedman, *Molecular quantum mechanics* (Oxford University Press, 2011).
- [21] K. T. Williams, Y. Yao, J. Li, L. Chen, H. Shi, M. Motta, C. Niu, U. Ray, S. Guo, R. J. Anderson, *et al.*, Phys. Rev. X **10**, 011041 (2020).
- [22] K. Langanke, J. A. Maruhn, and S. E. Koonin, *Computational nuclear physics* (Springer, 1991).
- [23] S. C. Pieper and R. B. Wiringa, Annu. Rev. Nucl. Part. Sci. **51**, 53 (2001).
- [24] K. Hebeler, S. Bogner, R. Furnstahl, A. Nogga, and A. Schwenk, Phys. Rev. C **83**, 031301 (2011).
- [25] A. Bazavov, D. Toussaint, C. Bernard, J. Laiho, C. Detar, L. Levkova, M. Oktay, S. Gottlieb, U. Heller, J. Hetrick, *et al.*, Rev. Mod. Phys. **82**, 1349 (2010).
- [26] J. Carlson, S. Gandolfi, F. Pederiva, S. C. Pieper, R. Schiavilla, K. Schmidt, and R. B. Wiringa, Rev. Mod. Phys. **87**, 1067 (2015).
- [27] N. Laflorencie and D. Poiblanc, “Quantum magnetism. lecture notes in physics,” (Springer-Verlag, 2004) Chap. Simulations of pure and doped low-dimensional spin-1/2 gapped systems.
- [28] R. M. Noack and S. R. Manmana, AIP Conf. Proc. **789**, 93 (2005).
- [29] A. Läuchli, “Introduction to frustrated magnetism: Materials, experiments, theory,” (Springer, 2011) Chap. Numerical Simulations of Frustrated Systems, pp. 481 – 511.
- [30] Reaching even these system sizes is possible only if internal, translation, and point group symmetries are utilized, and if state-of-the-art algorithms and large-scale computational resources are employed. Researchers usually employ much smaller systems for computational convenience.
- [31] S. R. White, Phys. Rev. Lett. **69**, 2863 (1992).
- [32] K. A. Hallberg, Adv. Phys. **55**, 477 (2006).
- [33] U. Schollwöck, Ann. Phys. **326**, 96 (2011).
- [34] E. M. Stoudenmire and S. R. White, Annu. Rev. Condens. Matter Phys. **3**, 111 (2012).
- [35] R. Ors, Ann. Phys. **349**, 117 (2014).
- [36] M. P. Nightingale and C. J. Umrigar, eds., *Quantum Monte Carlo Methods in Physics and Chemistry* (Springer, 1999).
- [37] A. M. Childs, D. Maslov, Y. Nam, N. J. Ross, and Y. Su, Proc. Natl. Acad. Sci. **115**, 9456 (2018).
- [38] I. Bloch, J. Dalibard, and S. Nascimbene, Nat. Phys. **8**, 267 (2012).
- [39] R. Blatt and C. F. Roos, Nat. Phys. **8**, 277 (2012).
- [40] E. Altman, K. R. Brown, G. Carleo, L. D. Carr, E. Demler, C. Chin, B. DeMarco, S. E. Economou, M. A. Eriksson, K.-M. C. Fu, *et al.*, arXiv:1912.06938 (2019).
- [41] J. Bausch, T. S. Cubitt, A. Lucia, D. Perez-Garcia, and M. M. Wolf, Proc. Natl. Acad. Sci. U.S.A **115**, 19 (2018).
- [42] J. Zeiher, R. van Bijnen, P. Schauß, S. Hild, J.-Y. Choi, T. Pohl, I. Bloch, and C. Gross, Nat. Phys. **12**, 1095 (2016).
- [43] N. Takei, C. Sommer, C. Genes, G. Pupillo, H. Goto, K. Koyasu, H. Chiba, M. Weidemüller, and K. Ohmori, Nature Communications **7**, 13449 (2016).
- [44] H. Bernien, S. Schwartz, A. Keesling, H. Levine, A. Omran, H. Pichler, S. Choi, A. S. Zibrov, M. Endres, M. Greiner, *et al.*, Nature **551**, 579 (2017).
- [45] E. Guardado-Sanchez, P. T. Brown, D. Mitra, T. Devakul, D. A. Huse, P. Schauß, and W. S. Bakr, Phys. Rev. X **8**, 021069 (2018).
- [46] V. Lienhard, S. de Léséleuc, D. Barredo, T. Lahaye, A. Browaeys, M. Schuler, L.-P. Henry, and A. M. Läuchli, Phys. Rev. X **8**, 021070 (2018).
- [47] A. P. Orioli, A. Signoles, H. Wildhagen, G. Günter, J. Berges, S. Whitlock, and M. Weidemüller, Phys. Rev. Lett. **120**, 063601 (2018).
- [48] B. Yan, S. A. Moses, B. Gadway, J. P. Covey, K. R. A. Hazzard, A. M. Rey, D. S. Jin, and J. Ye, Nature **501**, 521 (2013).

- [49] K. R. A. Hazzard, B. Gadway, M. Foss-Feig, B. Yan, S. A. Moses, J. P. Covey, N. Y. Yao, M. D. Lukin, J. Ye, D. S. Jin, and A. M. Rey, *Phys. Rev. Lett.* **113**, 195302 (2014).
- [50] F. Seeßelberg, X.-Y. Luo, M. Li, R. Bause, S. Kotochigova, I. Bloch, and C. Gohle, *Phys. Rev. Lett.* **121**, 253401 (2018).
- [51] S. Smale, P. He, B. A. Olsen, K. G. Jackson, H. Sharum, S. Trotzky, J. Marino, A. M. Rey, and J. H. Thywissen, *Sci. Adv.* **5** (2019), 10.1126/sciadv.aax1568.
- [52] A. De Paz, A. Sharma, A. Chotia, E. Marechal, J. Huckans, P. Pedri, L. Santos, O. Gorceix, L. Vernac, and B. Laburthe-Tolra, *Phys. Rev. Lett.* **111**, 185305 (2013).
- [53] C. Meldgin, U. Ray, P. Russ, D. Chen, D. M. Ceperley, and B. DeMarco, *Nat. Phys.* **12**, 646 (2016).
- [54] J.-Y. Choi, S. Hild, J. Zeiher, P. Schauß, A. Rubio-Abadal, T. Yefsah, V. Khemani, D. A. Huse, I. Bloch, and C. Gross, *Science* **352**, 1547 (2016).
- [55] P. Bordia, H. Lüschen, S. Scherg, S. Gopalakrishnan, M. Knap, U. Schneider, and I. Bloch, *Phys. Rev. X* **7**, 041047 (2017).
- [56] L. Gabardos, B. Zhu, S. Lepoutre, A. M. Rey, B. Laburthe-Tolra, and L. Vernac, arXiv:2005.13487 (2020).
- [57] A. Goban, R. B. Hutson, G. E. Marti, S. L. Campbell, M. A. Perlin, P. S. Julienne, J. P. D’Incao, A. M. Rey, and J. Ye, *Nature* **563**, 369 (2018).
- [58] J. Eisert, M. Friesdorf, and C. Gogolin, *Nat. Phys.* **11**, 124 (2015).
- [59] R. Nandkishore and D. A. Huse, *Annu. Rev. Condens. Matter Phys.* **6**, 15 (2015).
- [60] D. J. Luitz, N. Laflorencie, and F. Alet, *Phys. Rev. B* **93**, 060201 (2016).
- [61] D. J. Luitz and Y. B. Lev, *Ann. Phys. (Berlin)* **529**, 1600350 (2017).
- [62] S. A. Parameswaran and R. Vasseur, *Rep. Prog. Phys.* **81**, 082501 (2018).
- [63] T. Mori, T. N. Ikeda, E. Kaminishi, and M. Ueda, *J. Phys. B* **51**, 112001 (2018).
- [64] C.-M. Schmied, A. N. Mikheev, and T. Gasenzer, arXiv:1810.08143.
- [65] J. Simon, W. S. Bakr, R. Ma, M. E. Tai, P. M. Preiss, and M. Greiner, *Nature* **472**, 307 (2011).
- [66] S. Bravyi, M. B. Hastings, and F. Verstraete, *Phys. Rev. Lett.* **97**, 050401 (2006).
- [67] M. B. Hastings, arXiv:1008.5137 (2010).
- [68] E. H. Lieb and D. W. Robinson, *Commun. Math. Phys.* **28**, 251 (1972).
- [69] T. J. Osborne, *Phys. Rev. Lett.* **97**, 157202 (2006).
- [70] T. J. Osborne, *Phys. Rev. A* **75**, 032321 (2007).
- [71] T. J. Osborne, *Phys. Rev. A* **75**, 042306 (2007).
- [72] M. Kliesch, C. Gogolin, and J. Eisert, in *Many-Electron Approaches in Physics, Chemistry and Mathematics* (Springer, 2014) pp. 301–318.
- [73] M. P. Woods, M. Cramer, and M. B. Plenio, *Phys. Rev. Lett.* **115**, 130401 (2015).
- [74] M. P. Woods and M. B. Plenio, *J. Math. Phys.* **57**, 022105 (2016).
- [75] J. Haah, M. Hastings, R. Kothari, and G. H. Low, in *2018 IEEE 59th Annual Symposium on Foundations of Computer Science (FOCS)* (IEEE, 2018) pp. 350–360.
- [76] M. C. Tran, A. Y. Guo, Y. Su, J. R. Garrison, Z. Eldredge, M. Foss-Feig, A. M. Childs, and A. V. Gorshkov, *Phys. Rev. X* **9**, 031006 (2019).
- [77] C.-F. Chen and A. Lucas, arXiv preprint arXiv:1905.03682 (2019).
- [78] Z. Wang and K. R. Hazzard, *PRX Quantum* **1**, 010303 (2020).
- [79] D. Iyer, M. Srednicki, and M. Rigol, *Phys. Rev. E* **91**, 062142 (2015).
- [80] While the fact that the error bound for PBC is smaller than that for OBC does not necessarily imply that the actual finite size error in PBC is smaller, in the Supplemental Material [91] we use short-time perturbative arguments to show that the actual error in PBC is indeed smaller at early times for most initial product states.
- [81] M. B. Hastings and T. Koma, *Commun. Math. Phys.* **265**, 781 (2006).
- [82] J. Eisert, M. van den Worm, S. R. Manmana, and M. Kastner, *Phys. Rev. Lett.* **111**, 260401 (2013).
- [83] P. Richerme, Z.-X. Gong, A. Lee, C. Senko, J. Smith, M. Foss-Feig, S. Michalakis, A. V. Gorshkov, and C. Monroe, *Nature* **511**, 198 (2014).
- [84] Z.-X. Gong, M. Foss-Feig, S. Michalakis, and A. V. Gorshkov, *Phys. Rev. Lett.* **113**, 030602 (2014).
- [85] M. Foss-Feig, Z.-X. Gong, C. W. Clark, and A. V. Gorshkov, *Phys. Rev. Lett.* **114**, 157201 (2015).
- [86] T. Matsuta, T. Koma, and S. Nakamura, *Ann. Henri Poincaré* **18**, 519 (2017).
- [87] D. V. Else, F. Machado, C. Nayak, and N. Y. Yao, *Phys. Rev. A* **101**, 022333 (2020).
- [88] C.-F. Chen and A. Lucas, *Phys. Rev. Lett.* **123**, 250605 (2019).
- [89] T. Kuwahara and K. Saito, *Phys. Rev. X* **10**, 031010 (2020).
- [90] M. C. Tran, C.-F. Chen, A. Ehrenberg, A. Y. Guo, A. Deshpande, Y. Hong, Z.-X. Gong, A. V. Gorshkov, and A. Lucas, *Phys. Rev. X* **10**, 031009 (2020).
- [91] See Supplemental Material for the comparison of the error bounds to perturbation theory at early times, the detailed derivation of the PBC error bound in Eq. (6), and detailed derivations and expressions for the three different methods to bound the rhs of Eq. (6). The numerically tightest one is given in Eq. (S11), a more efficiently computable one is given in Eq. (S30), and the constants for the simplest one Eq. (7) are given in Eqs. (S43,S44,S46).
- [92] M. Vojta, *Rep. Prog. Phys.* **66**, 2069 (2003).
- [93] S. Sachdev, “Quantum phase transitions,” in *Handbook of Magnetism and Advanced Magnetic Materials* (American Cancer Society, 2007) <https://onlinelibrary.wiley.com/doi/pdf/10.1002/9780470022184.htm>
- [94] R. Coldea, D. A. Tennant, E. M. Wheeler, E. Wawrzynska, D. Prabhakaran, M. Telling, K. Habicht, P. Smeibidl, and K. Kiefer, *Science* **327**, 177 (2010).
- [95] J. Simon, W. S. Bakr, R. Ma, M. E. Tai, P. M. Preiss, and M. Greiner, *Nature* **472**, 307 (2011).
- [96] H. Labuhn, D. Barredo, S. Ravets, S. De Léséleuc, T. Macrì, T. Lahaye, and A. Browaeys, *Nature* **534**, 667 (2016).
- [97] E. Guardado-Sanchez, P. T. Brown, D. Mitra, T. Devakul, D. A. Huse, P. Schauß, and W. S. Bakr, *Phys. Rev. X* **8**, 021069 (2018).
- [98] A. Friedenauer, H. Schmitz, J. T. Glueckert, D. Porras, and T. Schätz, *Nat. Phys.* **4**, 757 (2008).
- [99] K. Kim, M.-S. Chang, S. Korenblit, R. Islam, E. E. Edwards, J. K. Freericks, G.-D. Lin, L.-M. Duan, and C. Monroe, *Nature* **465**, 590 (2010).
- [100] K. Kim, S. Korenblit, R. Islam, E. Edwards, M. Chang,

- C. Noh, H. Carmichael, G. Lin, L. Duan, C. J. Wang, *et al.*, *New J. Phys.* **13**, 105003 (2011).
- [101] B. P. Lanyon, C. Hempel, D. Nigg, M. Müller, R. Geritsma, F. Zähringer, P. Schindler, J. T. Barreiro, M. Rambach, G. Kirchmair, *et al.*, *Science* **334**, 57 (2011).
- [102] J. W. Britton, B. C. Sawyer, A. C. Keith, C.-C. J. Wang, J. K. Freericks, H. Uys, M. J. Biercuk, and J. J. Bollinger, *Nature* **484**, 489 (2012).
- [103] R. Barends, A. Shabani, L. Lamata, J. Kelly, A. Mezzacapo, U. Las Heras, R. Babbush, A. G. Fowler, B. Campbell, Y. Chen, *et al.*, *Nature* **534**, 222 (2016).
- [104] R. Harris, Y. Sato, A. Berkley, M. Reis, F. Altomare, M. Amin, K. Boothby, P. Bunyk, C. Deng, C. Enderud, *et al.*, *Science* **361**, 162 (2018).
- [105] J. Dziarmaga, *Phys. Rev. Lett.* **95**, 245701 (2005).
- [106] V. I. Anisimov, J. Zaanen, and O. K. Andersen, *Phys. Rev. B* **44**, 943 (1991).
- [107] T. Esslinger, *Annu. Rev. Condens. Matter Phys.* **1**, 129 (2010).
- [108] M. F. Parsons, A. Mazurenko, C. S. Chiu, G. Ji, D. Greif, and M. Greiner, *Science* **353**, 1253 (2016).
- [109] M. Boll, T. A. Hilker, G. Salomon, A. Omran, J. Nespolo, L. Pollet, I. Bloch, and C. Gross, *Science* **353**, 1257 (2016).
- [110] A. Mazurenko, C. S. Chiu, G. Ji, M. F. Parsons, M. Kanász-Nagy, R. Schmidt, F. Grusdt, E. Demler, D. Greif, and M. Greiner, *Nature* **545**, 462 (2017).
- [111] P. T. Brown, D. Mitra, E. Guardado-Sanchez, R. Nourafkan, A. Reymbaut, C.-D. Hébert, S. Bergeron, A.-M. Tremblay, J. Kokoalj, D. A. Huse, *et al.*, *Science* **363**, 379 (2019).
- [112] D. Pertot, A. Sheikhan, E. Cocchi, L. Miller, J. Bohn, M. Koschorreck, M. Köhl, and C. Kollath, *Phys. Rev. Lett.* **113**, 170403 (2014).
- [113] N. Schuch, S. K. Harrison, T. J. Osborne, and J. Eisert, *Phys. Rev. A* **84**, 032309 (2011)

Supplemental Material for “Bounding the finite-size error of quantum many-body dynamics simulations”

Zhiyuan Wang, Michael Foss-Feig, and Kaden R. A. Hazzard

The supplemental material fills in technical details for the refinements of the basic results in the main text. We first compare our error bounds to perturbation theory at early times and show that they are qualitatively tight for a large class of initial states, i.e. they grow with time as t^a with the correct exponent a . Next we give a detailed derivation of the improved error bound in PBC given in Eq. (6). Then we give three different methods to numerically upper bound the LR commutator that appears in the rhs of Eq. (6). The first one is to evaluate the series in Eq. (S11), which combines the methods in Refs. [77, 78]. This leads to the tightest bound, but is only efficiently computable in special cases. The second one is to numerically solve the differential equation (S21) and then calculate Eq. (S30). This method (which is based on Ref. [78]) is only slightly looser than the first one but is computationally efficient in general. The third method makes further simplifications which result in the simple analytic expression in Eq. (7), whose constants are given in Eqs. (S43,S44,S46). We emphasize that for any desired system, one may compute the LR bound and use it in the error formulas Eqs. (4) and (6). In this way, as LR bounds are refined in the future or extended to more general systems (e.g. long-range interacting [88–90], bosonic [113], or continuum ones), these refinements can immediately be used in the finite-size error bounds.

Comparison of finite-size error bounds to perturbation theory at early times

We can gain insights into the accuracy of our error bounds by comparing them to the true finite-size error at lowest order in time. We can do this analytically using the Taylor series expansion of the true finite-size error. Recall from Eq. (2) that finite-size error is defined as

$$\delta\langle\hat{S}(t)\rangle_\psi \equiv |\langle e^{i\hat{H}_L t}\hat{S}e^{-i\hat{H}_L t}\rangle_{\psi_L} - \langle e^{i\hat{H}t}\hat{S}e^{-i\hat{H}t}\rangle_\psi|, \quad (\text{S1})$$

where \hat{H}_L is the L -site finite Hamiltonian and ψ_L is the initial product state restricted to this finite chain. The Taylor series expansion of the time evolved operators can be expressed as sums of Lie clusters (nested commutators) involving \hat{S} and terms in the Hamiltonian [see, e.g. Eq. (S3)]. Many small clusters appear in both $\langle e^{i\hat{H}_L t}\hat{S}e^{-i\hat{H}_L t}\rangle_{\psi_L}$ and $\langle e^{i\hat{H}t}\hat{S}e^{-i\hat{H}t}\rangle_\psi$ and therefore cancel each other. Only those clusters whose spatial length is at least half of the system size may contribute to finite-size error. In the following we treat OBC and PBC separately, starting with OBC.

In OBC, finite-size error is due to those nested commutators in $\langle e^{-i\hat{H}t}\hat{S}e^{-i\hat{H}t}\rangle_\psi$ in which boundary terms appear at least once, since only such clusters are not canceled by any cluster in $\langle e^{-i\hat{H}_L t}\hat{S}e^{-i\hat{H}_L t}\rangle_{\psi_L}$. The lowest order cluster containing at least a boundary term is proportional to $\langle\hat{C}(\hat{S},\hat{V}_j)\rangle_\psi t^{D(\hat{S},\hat{V}_j)}/D(\hat{S},\hat{V}_j)!$, where \hat{V}_j the boundary term closest to \hat{S} , and $\hat{C}(\hat{S},\hat{V}_j)$ is the shortest nested commutator joining \hat{S} and \hat{V}_j . Assuming that the expectation value $\langle\hat{C}(\hat{S},\hat{V}_j)\rangle_\psi$ does not vanish (which is true for most initial product states $|\psi\rangle$), the true finite-size error has the same t dependence as the bound Eq. (5).

In PBC there is a qualitative difference. Any term in the Taylor expansion of $\langle e^{i\hat{H}t}\hat{S}e^{-i\hat{H}t}\rangle_\psi$ in Eq. (S1) whose spatial span is smaller than L do not contribute to finite size error, because they cancel the corresponding terms in $\langle e^{i\hat{H}_L t}\hat{S}e^{-i\hat{H}_L t}\rangle_{\psi_L}$ due to translation invariance and the product nature of the initial state, as shown in Fig. S1. Only those terms in $\langle e^{i\hat{H}t}\hat{S}e^{-i\hat{H}t}\rangle_\psi$ which are too long to be embeddable into an L -site periodic system can contribute. More precisely, in PBC, the rhs of Eq. (S1) is contributed by the following two classes of terms:

- (1) terms in $\langle e^{i\hat{H}t}\hat{S}e^{-i\hat{H}t}\rangle_\psi$ whose spatial span is larger than L , i.e. terms that are too long to be embeddable in the L -site PBC chain;
- (2) terms in $\langle e^{i\hat{H}_L t}\hat{S}e^{-i\hat{H}_L t}\rangle_{\psi_L}$ which wrap around the whole periodic system (wraps around the torus, or the circle in $d = 1$). Such terms do not generally cancel any terms in $\langle e^{i\hat{H}t}\hat{S}e^{-i\hat{H}t}\rangle_\psi$.

The leading order term in both classes are proportional to $t^\mathcal{L}$, where \mathcal{L} is the number of Hamiltonian terms in the smallest L -site-unembeddable cluster starting from \hat{S} . This $t^\mathcal{L}$ behavior is the same as the improved PBC bound in Eq. (7), and the exponent \mathcal{L} is roughly twice as large as the OBC exponent $D(\hat{S},\hat{V}_j)$. In the next section, we give a rigorous bound for the sum of all terms in each class.

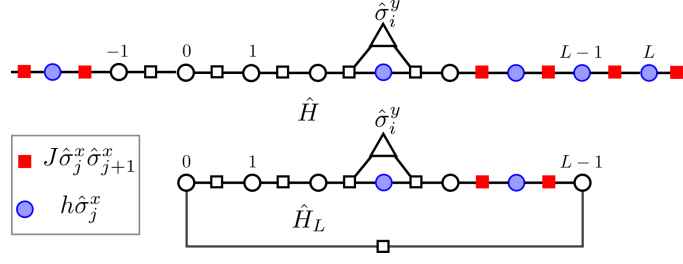


FIG. S1. An example of canceling terms in the Taylor expansions of $e^{i\hat{H}t}\hat{\sigma}_i^ye^{-i\hat{H}t}$ and $e^{i\hat{H}_Lt}\hat{\sigma}_i^ye^{-i\hat{H}_Lt}$, in the case of 1D TFIM. Vertices represent terms \hat{h}_j of the Hamiltonian $\hat{H} = \sum_j \hat{h}_j$, as well as the observable $\hat{S} = \hat{\sigma}_i^y$, and edges are drawn between terms that do not commute. The spatial span of the two Lie clusters shown in this figure (cluster of open circles, squares, and triangles) are equal and shorter than the system size. The expectation values of these two terms exactly cancel due to translation invariance and the initial state being a product state.

IMPROVED BOUND FOR PBC

For simplicity, we first focus on the one-dimensional (1D) case, and later we show that a bound in higher dimension can be obtained by repeatedly using the 1D bound. Consider a translation invariant quantum system on a 1D periodic lattice with L unit cells, described by the Hamiltonian \hat{H}_L , and let $\hat{H} = \hat{H}_{L \rightarrow \infty}$ be the Hamiltonian in the thermodynamic limit. We will derive an upper bound for the sum of all terms in $e^{-i\hat{H}t}\hat{S}e^{-i\hat{H}t}$ that may contribute to the finite-size error (i.e. whose spatial span is larger than L), using ideas motivated by Ref. [77], and then do the same for $e^{-i\hat{H}_Lt}\hat{S}e^{-i\hat{H}_Lt}$.

Let us focus on the first class of terms, i.e. terms in $e^{i\hat{H}t}\hat{S}e^{-i\hat{H}t}$ whose spatial span is larger than L , since the second class can be treated in an identical way. We write the Hamiltonian in the thermodynamic limit as

$$\hat{H} = \sum_{j \in G} \hat{h}_j, \quad (\text{S2})$$

where \hat{h}_j denotes a local term in \hat{H} . It is convenient to introduce the notion of the commutativity graph G , defined in Ref. [78]. This is a graph whose vertices j are associated with \hat{h}_j and which has edges from j to j' if and only if \hat{h}_j and $\hat{h}_{j'}$ do not commute. The observable \hat{S} is represented as an external vertex s on G , linked to all the vertices j whose \hat{h}_j do not commute with \hat{S} , as shown in Fig. S1. Now we write down the Taylor expansion of $e^{i\hat{H}t}\hat{S}e^{-i\hat{H}t}$. We use bold letters $\mathbf{h}_j = \text{ad}_{\hat{h}_j}$ to denote the adjoint of the corresponding operator \hat{h}_j , e.g. $\mathbf{h}_j(\hat{S}) \equiv [\hat{h}_j, \hat{S}]$. We have

$$\begin{aligned} e^{i\hat{H}t}\hat{S}e^{-i\hat{H}t} &= e^{i\mathbf{H}t}(\hat{S}) \\ &= \sum_{n=0}^{\infty} \frac{(it)^n}{n!} \sum_{\substack{j_1, \dots, j_n \in G \\ T(s, j_1, j_2, \dots, j_n) \in \mathcal{T}_s}} \mathbf{h}_{j_n} \dots \mathbf{h}_{j_2} \mathbf{h}_{j_1} \hat{S}, \end{aligned} \quad (\text{S3})$$

where $T(s, j_1, j_2, \dots, j_n)$ denotes the causal forest of the sequence $(s, j_1, j_2, \dots, j_n)$, as defined in Ref. [77], and \mathcal{T}_s denotes the set of causal trees starting from the vertex s . In simple terms, we are summing over all the non-vanishing connected Lie clusters on G starting from the vertex s .

Our goal is to upper bound the sum over all the terms in Eq. (S3) whose spatial span is larger than L . For such a Lie cluster, let j_i be the first term in the sequence j_1, \dots, j_n such that the spatial span of the subsequence $\mathbf{h}_{j_i} \dots \mathbf{h}_{j_1} \hat{S}$ is larger than L . This means that the spatial span of $\mathbf{h}_{j_{i-1}} \dots \mathbf{h}_{j_1} \hat{S}$ is less than or equal to L . We call j_i the *earliest unembeddable vertex* (EUV) of the sequence $(s, j_1, j_2, \dots, j_n)$. Notice that \hat{h}_{j_i} must act nontrivially on at least two unit cells, because otherwise j_i can never be the EUV of any sequence.

The basic idea is to classify the Lie clusters in Eq. (S3) into different families, with each family having the same EUV, and derive an upper bound for the sum over all terms within each family. To this end, let us denote by $[e^{i\mathbf{H}t}(\hat{S})]_k$ the sum of all the L -site unembeddable terms in the rhs of Eq. (S3) whose EUV is k , i.e.

$$[e^{i\mathbf{H}t}(\hat{S})]_k \equiv \sum_{\substack{n \geq 0, \\ T(s, j_1, j_2, \dots, j_n) \in \mathcal{T}_s, \\ \text{EUV}(s, j_1, j_2, \dots, j_n) = k}} \frac{(it)^n}{n!} \mathbf{h}_{j_n} \dots \mathbf{h}_{j_2} \mathbf{h}_{j_1} \hat{S}. \quad (\text{S4})$$

We limit our explicit proof to the nearest neighbor interacting case in which every term \hat{h}_j in the Hamiltonian acts non-trivially on at most two neighboring unit cells. The proof for the general case is the same as for the nearest-neighbor interacting case, but involves keeping track of more complicated notation. Therefore for the general case we omit the proof and present only the final result. Returning to the nearest-neighbor interacting case, for an arbitrary operator \hat{A} , let x_A^L, x_A^R denote the x -coordinates of the leftmost and rightmost unit cells on which the operator \hat{A} acts, and let $n_A \equiv x_A^R - x_A^L + 1$ denote the spatial span of \hat{A} (we write $x_k^{L,R}, n_k$ for the operator \hat{h}_k for simplicity). In the nearest neighboring interacting case, $n_k = 2$ if k is an EUV. Without loss of generality, let us suppose that $x_k^L < x_S^L$ (the other case $x_k^R > x_S^R$ can be treated similarly). In this case we need to have $x_S^R \leq x_k^R + L - 1$, because otherwise the cluster is already unembeddable before \hat{h}_k is attached, contradicting the assumption that k is the EUV. Then we have the following theorem:

Theorem 1.

$$[e^{i\mathbf{H}t}(\hat{S})]_k = i \int_0^t dt' e^{i\mathbf{H}(t-t')} \mathbf{h}_k (e^{i\mathbf{H}'_k t'} \hat{S} - e^{i\mathbf{H}_k t'} \hat{S}), \quad (\text{S5})$$

where

$$\hat{H}'_k = \hat{H}_{[x_k^L+1, \dots, x_k^L+L]}, \quad \hat{H}_k = \hat{H}_{[x_k^L+1, \dots, x_k^L+L-1]}, \quad (\text{S6})$$

where $\hat{H}_{[x_k^L+1, \dots, x_k^L+L]}$ denotes the truncation of \hat{H} to sites $[x_k^L + 1, \dots, x_k^L + L]$, and similarly for $\hat{H}_{[x_k^L+1, \dots, x_k^L+L-1]}$.

Thm. (1) can be proved by Taylor expanding both sides and explicitly comparing terms, using the same spirit as the proof of Lemma 5 and Lemma 6 in Ref. [77]. Intuitively, $e^{i\mathbf{H}'_k t'} \hat{S}$ gives the sum of all terms in the Taylor expansion of $e^{i\mathbf{H}t'} \hat{S}$ that act inside the region $[x_k^L + 1, \dots, x_k^L + L]$, so $(e^{i\mathbf{H}'_k t'} \hat{S} - e^{i\mathbf{H}_k t'} \hat{S})$ gives the sum of all terms in $e^{i\mathbf{H}t'} \hat{S}$ that act inside the region $[x_k^L + 1, \dots, x_k^L + L]$ and act non-trivially on $x_k^L + L$, since those terms which do not act on $x_k^L + L$ are canceled by $-e^{i\mathbf{H}_k t'} \hat{S}$. Further, only those terms in $(e^{i\mathbf{H}'_k t'} \hat{S} - e^{i\mathbf{H}_k t'} \hat{S})$ that act non-trivially on $x_k^R = x_k^L + 1$ can survive the commutation with \hat{h}_k in the rhs of Eq. (S5). In short, the surviving terms in $(e^{i\mathbf{H}'_k t'} \hat{S} - e^{i\mathbf{H}_k t'} \hat{S})$ are those terms that span exactly L unit cells $[x_k^R, \dots, x_k^L + L]$, which are the terms in $e^{i\mathbf{H}t'} \hat{S}$ that are L -site embeddable but become unembeddable immediately after attaching \mathbf{h}_k . Therefore the rhs of Eq. (S5) gives the sum of all Lie clusters in $e^{i\mathbf{H}t}(\hat{S})$ with k being the EUV, since the action of $e^{i\mathbf{H}(t-t')}$ happens at a time later than t' and can not change the earliestness of \hat{h}_k . [The last sentence can be better understood by noticing that $i \int_0^t dt' e^{i\mathbf{H}(t-t')} \mathbf{h}_k e^{i(\mathbf{H}-\mathbf{h}_k)t'} \hat{S}$ simply gives the sum of all terms in $e^{i\mathbf{H}t} \hat{S}$ in which \hat{h}_k appears at least once, with the \hat{h}_k at time t' being the earliest appearance. Therefore it is natural to expect that $i \int_0^t dt' e^{i\mathbf{H}(t-t')} \mathbf{h}_k (e^{i\mathbf{H}'_k t'} \hat{S} - e^{i\mathbf{H}_k t'} \hat{S})$ gives a subset of the terms in $i \int_0^t dt' e^{i\mathbf{H}(t-t')} \mathbf{h}_k e^{i(\mathbf{H}-\mathbf{h}_k)t'} \hat{S}$, whose EUV is k .]

For more general locally interacting Hamiltonians which involve terms that act non-trivially on more than 2 neighboring unit cells, Thm. (1) is generalized to

$$[e^{i\mathbf{H}t}(\hat{S})]_k = i \sum_{\alpha=1}^{n_k-1} \int_0^t dt' e^{i\mathbf{H}(t-t')} \mathbf{h}_k (e^{i\mathbf{H}'_{k,\alpha} t'} \hat{S} - e^{i\mathbf{H}_{k,\alpha} t'} \hat{S}), \quad (\text{S7})$$

where

$$\hat{H}'_{k,\alpha} = \hat{H}_{[x_k^L+\alpha, \dots, x_k^L+\alpha+L-1]}, \quad \hat{H}_{k,\alpha} = \hat{H}_{[x_k^L+\alpha, \dots, x_k^L+\alpha+L-2]}. \quad (\text{S8})$$

We can get an upper bound for the operator norm of the rhs of Eq. (S7) using the triangle inequality and unitary invariance of operator norm. The result is

$$\|e^{i\mathbf{H}t} \hat{S}|_{\text{span}>L}\| \leq \sum_{k,\alpha} \int_0^t dt' \|\hat{h}_k, e^{i\mathbf{H}'_{k,\alpha} t'}(\hat{S}) - e^{i\mathbf{H}_{k,\alpha} t'}(\hat{S})\|. \quad (\text{S9})$$

The second class of terms [those arising from $e^{i\mathbf{H}_k t}(\hat{S})$] can be bounded in a similar way, and it turns out that the resulting upper bound for the second class is identical to the first class, Eq. (S9). Adding up the two classes and taking $n_k = 2$, we get Eq. (6) in the main text.

In the following we give two different approaches to upper bound the commutator in the rhs of Eq. (S9). The first one is based on a combination of the methods in Ref. [77, 78]. This method leads to the tightest bound but has a high computational cost (potentially exponential in the system size) except in a few simple cases. The second one is based on the differential equation method in Ref. [78], which is slightly looser than the first one, but is much easier to compute, and can also lead to a simple analytic upper bound such as Eq. (7).

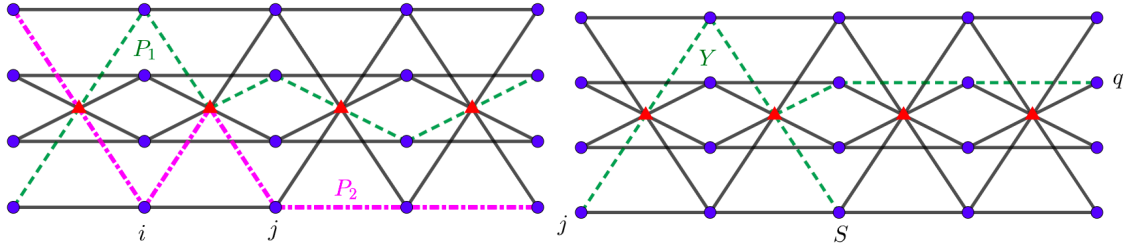


FIG. S2. Examples of irreducible path and Y -shape on the commutativity graph of the FHM. (Left) The dark green, dashed path P_1 is irreducible, while the pink, dot-dashed path P_2 is reducible since the pair (i, j) is not consecutive in P_2 but $(i, j) \in G$. (Right) Example of an irreducible Y -shape.

CHEN-LUCAS BOUND FOR LR COMMUTATORS

In this section we present the tightest LR bounds for locally interacting systems, obtained by applying the method in Ref. [77] to the commutativity graph introduced in Ref. [78]. The goal is to upper bound $\|\hat{h}_j, \hat{S}(t)\|$ which appears in the simple bound in Eq. (4) and $\|\hat{h}_k, e^{i\mathbf{H}_k t'}(\hat{S}) - e^{i\mathbf{H}_k t'}(\hat{S})\|$ which appears in the improved PBC bound in Eq. (S9). We begin with the first one. The bound for the second one is a generalization of the first one and is qualitatively smaller at early times. For simplicity we focus on 1D in this section.

The bound for $\|\hat{h}_j, \hat{S}(t)\|$ is obtained by generalizing Thm. 4 of Ref. [77] to the commutativity graph G . The result is (we present the time integrated version for simplicity)

$$\int_0^t \|\hat{h}_j, \hat{S}(t')\| dt' \leq \|\hat{S}\| \sum_{P \in \mathcal{P}_{jS}} \frac{(2t)^{n(P)-1}}{[n(P)-1]!} \prod_{i \in P, i \neq s} h_i, \quad (\text{S10})$$

where \mathcal{P}_{jS} is the set of all irreducible paths on G from S to j , $n(P)$ is the number of vertices in P , and $h_i = \|\hat{h}_i\|$. An irreducible path P on graph G is a simple path (a path without repeated vertices) in which any two non-consecutive vertices in P are not adjacent in G . That is, let $P = (i_n = j, i_{n-1}, i_{n-2}, \dots, i_2, i_1 = S)$, then we have $(i_m, i_{m-1}) \notin G$, $2 \leq m \leq n$. See Fig. S2 for examples of irreducible paths.

The bound for $\|\hat{h}_j, e^{i\mathbf{H}_j t'}(\hat{S}) - e^{i\mathbf{H}_j t'}(\hat{S})\|$ is obtained in a similar way:

$$\int_0^t \|\hat{h}_j, e^{i\mathbf{H}_j t'}(\hat{S}) - e^{i\mathbf{H}_j t'}(\hat{S})\| dt' \leq \|\hat{S}\| \sum_{\hat{H}_q \in \hat{H}'_j - \hat{H}_j} \sum_{Y \in \mathcal{Y}_{s,jq}} \binom{n_j(Y) + n_q(Y) - 1}{n_q(Y)} \frac{(2t)^{n(Y)-1}}{[n(Y)-1]!} \prod_{i \in Y, i \neq s} h_i, \quad (\text{S11})$$

where the first sum is over all vertices q that appears in $\hat{H}'_j - \hat{H}_j$, $\mathcal{Y}_{s,jq}$ is the set of all irreducible Y -shapes on G with root s and end points j, q , $n_j(Y)$ is the number of vertices on the j -branch of Y and similarly for $n_q(Y)$, so that $n(Y) = n_j(Y) + n_q(Y) + n_s(Y) + 1$. The definition of an irreducible Y -shape with root s and endpoints j, q generalizes that of an irreducible path: it is a three-branch tree with a branch point y (y may coincide with one of s, j, q) such that the three branches P_{sy}, P_{jy}, P_{qy} are irreducible paths, and any vertex in $P_{sy} \setminus \{y\}$ is not linked (with respect to G) to any vertex in $(P_{jy} \cup P_{qy}) \setminus \{y\}$. The binomial coefficient in Eq. (S11) arises due to the different ways of relative time ordering the operators on the j -branch and the q -branch of Y .

We can see that at early times, the improved PBC bound in Eq. (S11) grows like $t^{\min n(Y_s)-1}$, where the minimum is taken over all the L -cell-unembeddable Y -shapes with root s (notice that the set of smallest L -cell-unembeddable Y -shapes always contain an irreducible one). Put it another way, the small- t exponent of the improved PBC bound is equal to the minimum number of Hamiltonian terms needed to be attached to \hat{S} to make the cluster unembeddable (or, the number of Hamiltonian terms in the smallest unembeddable Lie cluster containing S), which agrees with perturbation theory (provided that the expectation value in $|\psi\rangle$ of the leading term doesn't vanish).

In general, the rhs of Eqs. (S10,S11) can only be calculated numerically. Yet there are a few special cases in which we can obtain simple analytic expressions due to the simple structure of the commutativity graph. In the following we show the bound for 1D TFIM as an example. Similar bounds apply to any 1D model whose commutativity graph is a single chain, another example is the FHM in the large- U limit [78].

Example: 1D TFIM in PBC We write the Hamiltonian as

$$\hat{H} = -J \sum_j \hat{Z}_{j,j+1} - h \sum_j \hat{X}_j, \quad (\text{S12})$$

where $\hat{Z}_{j,j+1} \equiv \hat{\sigma}_j^z \hat{\sigma}_{j+1}^z$ and $\hat{X}_j \equiv \hat{\sigma}_j^x$. For illustrative purpose, take $\hat{S} = \hat{\sigma}_i^x$. The commutativity graph G is simply a 1D ring, as shown in Fig. S1. In this case, there are only two irreducible paths between any two points in G . Inserting Eq. (S10) evaluated for the PBC TFIM into Eq. (4) we obtain

$$|\delta\langle\hat{\sigma}_j^x(t)\rangle_\psi| \leq 4\sqrt{\frac{J}{h}} \frac{(2\sqrt{Jht})^L}{L!} + 2\sqrt{\frac{J}{h}} \frac{(2\sqrt{Jht})^{L+2}}{(L+2)!}, \quad (\text{S13})$$

where we assume for simplicity that L is an odd integer.

The improved PBC error bound for $\delta\langle\hat{\sigma}_i^x(t)\rangle_\psi$ is given by Eq. (6), which in the current case becomes

$$|\delta\langle\hat{\sigma}_i^x(t)\rangle_\psi| \leq 2 \sum_{|j-i|\leq L} \int_0^t dt' \| [J\hat{Z}_{j,j+1}, e^{i\mathbf{H}'_j t'}(\hat{X}_i) - e^{i\mathbf{H}_j t'}(\hat{X}_i)] \|, \quad (\text{S14})$$

where $\hat{H}'_j = \hat{H}_{[j+1,\dots,j+L]}$, $\hat{H}_j = \hat{H}_{[j+1,\dots,j+L-1]}$ for $j < i$, and we have a similar expression for $j \geq i$. Now we apply Eq. (S11) to bound the rhs. In this case, $\hat{h}_q = JZ_{j+L-1,j+L}$, and since both \hat{H}'_j, \hat{H}_j have open boundary, there is only one irreducible Y -shape with endpoints j, s, q . Eq. (S11) becomes

$$\int_0^t dt' \| [J\hat{Z}_{j,j+1}, e^{i\mathbf{H}'_j t'}(\hat{X}_i) - e^{i\mathbf{H}_j t'}(\hat{X}_i)] \| \leq \frac{(2t)^{2L-2}}{(2L-2)!} J^L h^{L-2} \binom{2L-3}{n_j}, \quad n_j = \begin{cases} 2(i-j)-1, & i-L < j < i, \\ 2(j-i)+1, & i \leq j < i+L. \end{cases} \quad (\text{S15})$$

When $|j-i| = L$, we have $e^{i\mathbf{H}'_j t'}(\hat{X}_i) = \hat{X}_i$, so we can simply use Eq. (S10). The result is similar to the first term in Eq. (S13) with substitution $L \rightarrow 2L-1$. Inserting Eq. (S15) along with the $|j-i| = L$ case into Eq. (S14), we get

$$|\delta\langle\hat{\sigma}_j^x(t)\rangle| \leq 4\sqrt{\frac{J}{h}} \frac{(2\sqrt{Jht})^{2L-1}}{(2L-1)!} + \frac{J}{h} \frac{(4\sqrt{Jht})^{2L-2}}{(2L-2)!}. \quad (\text{S16})$$

BOUNDING THE PBC ERROR BOUND BY SOLVING A LINEAR DIFFERENTIAL EQUATION

Apart from a few special cases, the computational complexity of the Chen-Lucas bound, Eq. (S11), grows exponentially with system size, since the number of irreducible paths on G grows exponentially in general. For some models with very complicated G , the computation of the Chen-Lucas bound may take even longer than the quantum dynamics simulation itself. For this reason, in this section we give an alternative method based on Ref. [78], which is slightly looser than the Chen-Lucas bound but whose computational time complexity grows only quadratically with system size. In addition, with some further simplifications this method leads to the simple analytic expression in Eq. (7).

The goal here is to bound the finite-size error of a dynamics simulation on a periodic cluster of size $L_1 \times L_2 \times \dots \times L_d$. The first step is to extend the 1D bound to d dimensions. To this end, denote by \mathcal{C}_j a cluster of size $L_1 \times L_2 \times \dots \times L_j \times \infty \times \dots \times \infty$, that is, for $i \leq j$, the i -th direction is periodic with size L_i , while for $i > j$ the i -th direction is infinite. Then we have

$$\begin{aligned} |\delta\langle\hat{S}(t)\rangle_{L_1 \times \dots \times L_d}| &\equiv |\langle\hat{S}(t)\rangle_{\infty \times \dots \times \infty} - \langle\hat{S}(t)\rangle_{L_1 \times \dots \times L_d}| \\ &\leq \sum_{j=1}^d |\langle\hat{S}(t)\rangle_{\mathcal{C}_{j-1}} - \langle\hat{S}(t)\rangle_{\mathcal{C}_j}| \end{aligned} \quad (\text{S17})$$

Since for each j , the clusters \mathcal{C}_{j-1} and \mathcal{C}_j only differ in the j -th direction, the difference $|\langle\hat{S}(t)\rangle_{\mathcal{C}_{j-1}} - \langle\hat{S}(t)\rangle_{\mathcal{C}_j}|$ can be upper bounded using the 1D method. In the following we first focus on the $j=1$ term, since other terms can be treated in an almost identical way. As before, we mainly focus on the ‘‘nearest-neighbor interacting’’ case (only allow interactions between neighboring unit cells), as the generalization to non-nearest-neighbor interactions is straightforward. We have

$$|\langle\hat{S}(t)\rangle_{\mathcal{C}_0} - \langle\hat{S}(t)\rangle_{\mathcal{C}_1}| \leq 2 \int_0^t dt' \sum_k \| [\hat{h}_k, e^{i\mathbf{H}'_k t'}(\hat{S}) - e^{i\mathbf{H}_k t'}(\hat{S})] \|. \quad (\text{S18})$$

Notice that

$$\begin{aligned} [\hat{h}_k, e^{i\mathbf{H}'_k t}(\hat{S}) - e^{i\mathbf{H}_k t}(\hat{S})] &= \int_0^t dt' \mathbf{h}_k e^{i\mathbf{H}'_k t'} \frac{d}{dt'} (\hat{S} - e^{-i\mathbf{H}'_k t'} e^{i\mathbf{H}_k t'} \hat{S}) \\ &= i \int_0^t dt' \mathbf{h}_k e^{i\mathbf{H}'_k(t-t')} (\mathbf{H}'_k - \mathbf{H}_k) e^{i\mathbf{H}_k t'} (\hat{S}). \end{aligned} \quad (\text{S19})$$

Ref. [78] introduces a method to bound unequal time commutator of the form $\mathbf{h}_k e^{i\mathbf{H}t}(\hat{S})$ by solving a first order linear differential equation on the commutativity graph G . In the following we extend this method to bound double commutators of the form $\mathbf{h}_k e^{i\mathbf{H}_2(t-t')} \mathbf{h}_j e^{i\mathbf{H}_1 t'}(\hat{S})$, where $\hat{H}_2 = \hat{H}'_k$, $\hat{H}_1 = \hat{H}_k$, as required for Eq. (S19).

To begin, let us first recall some basic results from Ref. [78] and fix our notations. The thermodynamic limit Hamiltonian with commutativity graph G is written in Eq. (S2) as $\hat{H} = \sum_{j \in G} \hat{h}_j$. Since both \hat{H}_1 and \hat{H}_2 are sums of subset of terms in $\hat{H}_\infty = \hat{H}$ [see Eq. (S8)], we can write

$$\hat{H}_a = \sum_{j \in G} \hat{h}_j^a, \quad a = 1, 2, \infty, \quad (\text{S20})$$

where $\hat{h}_j^a = \hat{h}_j$ if the term \hat{h}_j is contained in \hat{H}_a and $\hat{h}_j^a = 0$ otherwise. Let $G_{ij}^a(t)$ be the solution to the differential equation

$$\frac{d}{dt} G_{ij}^a(t) = 2 \sum_{k: \langle ki \rangle \in G} \sqrt{h_i^a h_k^a} G_{kj}^a(t) \equiv \sum_{k \in G} M_{ik}^a G_{kj}^a, \quad a = 1, 2, \infty, \quad (\text{S21})$$

with initial condition $G_{ij}^a(0) = \delta_{ij}$, where $h_i^a \equiv \|\hat{h}_i^a\| \geq 0$ and $M_{ik}^a \equiv 2\sqrt{h_i^a h_k^a} \cdot (\langle ik \rangle \in G)$. The solutions can be written formally as $G_{ij}^a(t) = [e^{M^a t}]_{ij}$. Notice that since $0 \leq h_j^1 \leq h_j^2 \leq h_j$ we have $0 \leq M_{ij}^1 \leq M_{ij}^2 \leq M_{ij}$ and therefore $G_{ij}^1(t) \leq G_{ij}^2(t) \leq G_{ij}(t)$ for $t \geq 0$. In translation invariant systems, $G_{ij}(t)$ has a Fourier integral expression

$$G_{ij}(t) = [e^{Mt}]_{ij} = \int_{\vec{k}} [e^{M_{\vec{k}} t}]_{\alpha_i \alpha_j} e^{i\vec{k} \cdot (\vec{r}_i - \vec{r}_j)}, \quad (\text{S22})$$

where \vec{r}_i denotes the lattice translation vector of the unit cell containing vertex i , α_i labels the index of i inside a unit cell, we use the notation $\int_{\vec{k}} = \int \frac{d^d k}{(2\pi)^d}$, and

$$[M_{\vec{k}}]_{\alpha_i \alpha_j} \equiv \sum_{\vec{r}_j} M_{ij} e^{-i\vec{k} \cdot (\vec{r}_i - \vec{r}_j)}. \quad (\text{S23})$$

In the following we first upper bound $\|\mathbf{h}_k e^{i\mathbf{H}_2(t-t')} \mathbf{h}_j e^{i\mathbf{H}_1 t'}(\hat{S})\|$ in terms of $G_{ij}^a(t)$ and then apply Eq. (S22) to get a simple final expression.

First consider the case when $t' = t$. For an arbitrary local operator \hat{A} , denote $\hat{A}^i(t) = [\hat{h}_i, \hat{A}(t)]$ and $\hat{A}^{ij}(t) = [\hat{h}_i, [\hat{h}_j, \hat{A}(t)]]$, where $\hat{A}(t) \equiv e^{i\mathbf{H}_1 t}(\hat{A})$. We want to find an upper bound for $\|\hat{S}^{ij}(t)\|$. Taking the time derivative using Heisenberg's equation, we have [note: from Eq. (S24) to Eq. (S29) we write \hat{h}_j to mean \hat{h}_j^1 for notational simplicity]

$$\begin{aligned} i \frac{d}{dt} \hat{A}^{ij}(t) &= [\hat{h}_i, [\hat{h}_j, [\hat{A}(t), \sum_{k: \langle kA \rangle \in G} \hat{h}_k(t)]]] \\ &= \sum_{k: \langle kA \rangle \in G} \{ [\hat{A}^{ij}(t), \hat{h}_k(t)] + [\hat{A}(t), \hat{h}_k^{ij}(t)] + [\hat{A}^i(t), \hat{h}_k^j(t)] + [\hat{A}^j(t), \hat{h}_k^i(t)] \}. \end{aligned} \quad (\text{S24})$$

We can use the same derivations as in Eqs. (6-8) in Ref. [78] to prove that

$$\|\hat{A}^{ij}(t)\| \leq 2 \sum_{k: \langle kA \rangle \in G} \int_0^t \{ \|\hat{A}\| \|\hat{h}_k^{ij}(t')\| + \|\hat{A}^i(t')\| \|\hat{h}_k^j(t')\| + \|\hat{A}^j(t')\| \|\hat{h}_k^i(t')\| \} dt'. \quad (\text{S25})$$

The last two terms can be bounded by Eqs. (16,17) of Ref. [78]:

$$\|\hat{A}^i(t)\| \leq \bar{A}^i(t) \equiv \sum_{k: \langle kA \rangle \in G} G_{ik}^1(t) \sqrt{h_k h_i} 2 \|\hat{A}\|. \quad (\text{S26})$$

Notice that $\frac{d}{dt}\bar{A}^i(t) = \sum_{k:\langle kA \rangle \in G} 2\|A\|\bar{h}_k^i(t)$, so the last two terms in Eq. (S25) can be combined to $\frac{d}{dt'}[\bar{A}^i(t')\bar{A}^i(t')]/\|\hat{A}\|$, and we get

$$\|\hat{A}^{ij}(t)\| \leq 2 \sum_{k:\langle kA \rangle \in G} \int_0^t \|\hat{A}\| \|\hat{h}_k^{ij}(t')\| dt' + \bar{A}^i(t)\bar{A}^j(t)/\|\hat{A}\|. \quad (\text{S27})$$

Now take $\hat{A} = \hat{h}_l$, a term in \hat{H} . Using Grönwall's inequality, we can prove that $\|\hat{h}_l^{ij}(t)\| \leq \bar{h}_l^{ij}(t)$ where $\bar{h}_l^{ij}(t)$ is the solution to the differential equation

$$\frac{d}{dt}\bar{h}_l^{ij}(t) = 2 \sum_{k:\langle kl \rangle \in G} h_l \bar{h}_k^{ij}(t) + \frac{1}{h_l} \frac{d}{dt}[\bar{h}_l^i(t)\bar{h}_l^j(t)], \quad (\text{S28})$$

with initial condition $\bar{h}_l^{ij}(0) = 0$. If we substitute $\bar{\Gamma}_l(t) = \bar{h}_l^{ij}(t)/\sqrt{h_l}$, Eq. (S28) is of the form $\frac{d}{dt}\bar{\Gamma} = M^a \cdot \bar{\Gamma} + B$, which has formal solution $\bar{\Gamma}(t) = \int_0^t dt' e^{M^a(t-t')} B(t') dt'$, i.e.

$$\bar{h}_l^{ij}(t) = \sum_k \int_0^t \sqrt{\frac{h_l}{h_k^3}} G_{lk}^1(t-t') d[\bar{h}_k^i(t')\bar{h}_k^j(t')]. \quad (\text{S29})$$

An upper bound for $\|S^{ij}(t)\|$ can be obtained by taking $\hat{A} = \hat{S}$ in Eq. (S27) and inserting Eqs. (S26, S29). Finally, Eq. (15) in Ref. [78] allows us to upper bound $\|\mathbf{h}_i e^{i\mathbf{H}_2(t-t')} \mathbf{h}_j e^{i\mathbf{H}_1 t'}(\hat{S})\|$ in terms of $\|\hat{S}^{ij}(t)\|$ and $G_{ij}^2(t)$ by taking $\hat{B} = \mathbf{h}_j e^{i\mathbf{H} t'}(\hat{S})$:

$$\|\mathbf{h}_i e^{i\mathbf{H}_2(t-t')} \mathbf{h}_j e^{i\mathbf{H}_1 t'}(\hat{S})\| \leq 2 \sum_{l \in G} G_{il}^2(t-t') \sqrt{\frac{h_i}{h_l}} \|\hat{S}^{lj}(t')\|. \quad (\text{S30})$$

In summary, to get a bound for finite-size error $|\delta\langle \hat{S}(t) \rangle_{L_1 \times \dots \times L_d}|$, one need to first solve the differential equation Eq. (S21) to get $G_{ij}^1(t), G_{ij}^2(t)$ [note that since $G_{ij}^1(t) \leq G_{ij}^2(t)$, having a bound for $G_{ij}^2(t)$ is enough], then use Eqs. (S26, S27, S29) to get a bound for $\|\hat{S}^{lj}(t')\|$, then insert into Eq. (S30) to get a bound for the double commutator, and finally use Eqs. (S17, S18, S19) to bound $|\delta\langle \hat{S}(t) \rangle_{L_1 \times \dots \times L_d}|$. All steps in this procedure are efficient, with total computational cost scaling at most quadratically with the system size.

Derivation of Eq. (7)

We now derive the simple bound in Eq. (7). We use $G_{ij}^a(t) \leq G_{ij}(t)$ and Eq. (S22) to simplify the expression. Eq. (S29) becomes

$$\bar{h}_l^{ij}(t) = \sqrt{h_j h_j h_l} \sum_{m \in G} \int_0^t \frac{1}{\sqrt{h_m}} [e^{M(t-t')}]_{lm} [M^2 e^{Mt'}]_{im} [M e^{Mt'}]_{jm} dt' + (i \leftrightarrow j). \quad (\text{S31})$$

Taking $\hat{A} = \hat{S}$ in Eq. (S27) and inserting Eqs. (S26, S31), we get

$$\bar{S}^{ij}(t_3) = \sqrt{h_i h_j} \sum_{m, l \in G} \int_{t_{1,2}} \frac{S_l}{\sqrt{h_m}} [e^{M(t_2-t_1)}]_{lm} [M^2 e^{Mt_1}]_{im} [M e^{Mt_1}]_{jm} + (i \leftrightarrow j) + \bar{S}^i(t_3) \bar{S}^j(t_3)/S, \quad (\text{S32})$$

where $\int_{t_{1,2}} \equiv \int_{0 \leq t_1 \leq t_2 \leq t_3} dt_1 dt_2$ and $S_l \equiv 2\sqrt{h_l}(\langle ls \rangle \in G) \|\hat{S}\|$. Notice that M is symmetric, and so are $e^{Mt}, M e^{Mt}$, etc. Inserting Eq. (S32) into Eq. (S30), we obtain

$$\begin{aligned} \|\mathbf{h}_i e^{i\mathbf{H}_2(t-t_3)} \mathbf{h}_j e^{i\mathbf{H}_1 t_3}(\hat{S})\| &\leq 2 \int_{t_{1,2}} \sum_{\substack{m, l \in G \\ a=1,2}} \sqrt{\frac{h_i h_j}{h_m}} [M^{3-a} e^{M(t-t_3+t_2-t_1)}]_{im} [M^a e^{M(t_2-t_1)}]_{jm} [e^{Mt_1}]_{ml} S_l + 2\bar{S}^i(t) \bar{S}^j(t_3)/S \\ &= 2 \int_{t_{1,2}, \bar{k}_{1,2}} \sum_{\substack{\alpha_m, l \\ a=1,2}} \sqrt{\frac{h_i h_j}{h_m}} [M_{\bar{k}_1}^{3-a} e^{M_{\bar{k}_1}(t-t_3+t_2-t_1)}]_{\alpha_i \alpha_m} [M_{\bar{k}_2}^a e^{M_{\bar{k}_2}(t_2-t_1)}]_{\alpha_j \alpha_m} \\ &\quad \times [e^{M_{\bar{k}_1 + \bar{k}_2} t_1}]_{\alpha_m \alpha_i} e^{i\bar{k}_1 \cdot (\bar{r}_i - \bar{r}_l) + i\bar{k}_2 \cdot (\bar{r}_j - \bar{r}_l)} S_l + 2\bar{S}^i(t) \bar{S}^j(t_3)/S, \end{aligned} \quad (\text{S33})$$

where α_m runs over all vertices in a unit cell. Now we insert Eq. (S33) into Eqs. (S19) and (S18) to bound finite size error $|\langle \hat{S}(t) \rangle_{\mathcal{C}_0} - \langle \hat{S}(t) \rangle_{\mathcal{C}_1}|$. Eqs. (S19) and (S18) combines to be

$$|\langle \hat{S}(t) \rangle_{\mathcal{C}_0} - \langle \hat{S}(t) \rangle_{\mathcal{C}_1}| \leq 2 \sum_{(i,j) \in \mathcal{S}} \int_0^t dt_4 \int_0^{t_4} \|\mathbf{h}_i e^{i\mathbf{H}_2(t_4-t_3)} \mathbf{h}_j e^{i\mathbf{H}_1 t_3} (\hat{S})\| dt_3, \quad (\text{S34})$$

where

$$\begin{aligned} \mathcal{S} \equiv & \{(i,j) | n_i = n_j = 2 \wedge x_i^L < x_S^L \wedge x_S^R \leq x_i^R + L - 1 \wedge x_j^L = x_i^L + L - 1\} \\ & \cup \{(i,j) | n_i = n_j = 2 \wedge x_i^R > x_S^R \wedge x_S^L \geq x_i^L - (L - 1) \wedge x_j^R = x_i^R - (L - 1)\}. \end{aligned} \quad (\text{S35})$$

The restriction on the summation over (i,j) follows from the discussion above Thm. 1 and the definition of \hat{H}_i, \hat{H}'_i in Eq. (S6), which is essentially the requirement that i is the EUV of some Lie cluster starting from the vertex s , and that \hat{h}_j is a term in $\hat{H}_2 - \hat{H}_1 \equiv \hat{H}'_i - \hat{H}_i$. Notice that the set \mathcal{S} is translation invariant in directions L_2, \dots, L_d . Namely, if $(i,j) \equiv ((\vec{r}_i, \alpha_i), (\vec{r}_j, \alpha_j)) \in \mathcal{S}$, then for any $\vec{r}_{1\perp} \perp \hat{x}, \vec{r}_{2\perp} \perp \hat{x}$, we have $(i', j') \equiv ((\vec{r}_i + \vec{r}_{1\perp}, \alpha_i), (\vec{r}_j + \vec{r}_{2\perp}, \alpha_j)) \in \mathcal{S}$. Let \mathcal{T}_\perp denote the group of all lattice translation vectors in directions L_2, \dots, L_d , such that $\mathcal{S} \cong \mathcal{S}/\mathcal{T}_\perp \times \mathcal{T}_\perp$. We can therefore decompose the sum over i,j as $\sum_{(i,j) \in \mathcal{S}} = \sum_{(x_i, x_j) \in \mathcal{S}/\mathcal{T}_\perp} \sum_{(\vec{r}_{i\perp}, \vec{r}_{j\perp}) \in \mathcal{T}_\perp}$. We have (we abbreviate $x_i = x_i^L, x_j = x_j^L$)

$$\begin{aligned} \sum_{\substack{(\vec{r}_{i\perp}, \vec{r}_{j\perp}) \\ \in \mathcal{T}_\perp}} \|\mathbf{h}_i e^{i\mathbf{H}_2(t-t_3)} \mathbf{h}_j e^{i\mathbf{H}_1 t_3} (\hat{S})\| & \leq 2\sqrt{h_{\alpha_i} h_{\alpha_j}} \int_{t_1, 2, k_{1x}, k_{2x}} \sum_{\substack{\alpha_m, l \\ a=1, 2}} [M_{k_{1x}}^{3-a} e^{M_{k_{1x}}(t-t_3+t_2-t_1)}]_{\alpha_i \alpha_m} [M_{k_{2x}}^a e^{M_{k_{2x}}(t_2-t_1)}]_{\alpha_j \alpha_m} \\ & \times [e^{M_{k_{1x}+k_{2x}} t_1}]_{\alpha_m \alpha_l} \frac{1}{\sqrt{h_{\alpha_m}}} e^{ik_{1x}(x_i-x_l)+ik_{2x}(x_j-x_l)} S_l + 2\bar{S}_x^i(t) \bar{S}_x^j(t_3)/S, \end{aligned} \quad (\text{S36})$$

where $M_{k_x} \equiv M_{\vec{k}=(k_x, 0, \dots, 0)}$, and

$$\bar{S}_x^j(t) = \sum_{\vec{r}_{j\perp} \in \mathcal{T}_\perp} \bar{S}^j(t) = \sum_{\langle nS \rangle} \int_{k_x} [e^{M_{k_x} t}]_{\alpha_j \alpha_n} e^{ik_x(x_j-x_n)} 2\sqrt{h_j h_n} S. \quad (\text{S37})$$

We now need to sum over x_i, x_j satisfying restrictions defined in Eq. (S35). Notice that all such (x_i, x_j) satisfy $|x_i - x_j| = L - 1$. It turns out to be more convenient to extend the summation to all (x_i, x_j) satisfying $|x_i - x_j| = L - 1$. This still gives an upper bound since the rhs of Eq. (S33) is always non-negative. We let $x_j = x_i \pm (L - 1)$ and sum over x_i from $-\infty$ to ∞ :

$$\begin{aligned} \sum_{(i,j) \in \mathcal{S}} \|\mathbf{h}_i e^{i\mathbf{H}_2(t_4-t_3)} \mathbf{h}_j e^{i\mathbf{H}_1 t_3} (\hat{S})\| & \leq 2 \sum_{\substack{\alpha_m, \alpha_i, \alpha_j, l \\ a=1, 2 \\ \Delta x = \pm(L-1)}} \sqrt{h_{\alpha_i} h_{\alpha_j}} \int_{t_1, 2, k_x} [M_{-k_x}^{3-a} e^{M_{-k_x}(t_4-t_3+t_2-t_1)}]_{\alpha_i \alpha_m} [M_{k_x}^a e^{M_{k_x}(t_2-t_1)}]_{\alpha_j \alpha_m} \\ & \times [e^{M_0 t_1}]_{\alpha_m \alpha_l} \frac{1}{\sqrt{h_{\alpha_m}}} e^{ik_x \Delta x} S_l + \sum_{(i,j) \in \mathcal{S}/\mathcal{T}_\perp} 2\bar{S}_x^i(t_4) \bar{S}_x^j(t_3)/S. \end{aligned} \quad (\text{S38})$$

This is the bound for the $j = 1$ term in Eq. (S17). Those $j > 1$ terms in Eq. (S17) can be treated in an almost identical way; the only difference is that since the directions L_1, \dots, L_{j-1} are now periodic, the integrals over \vec{k} in those $j - 1$ directions have to be replaced by a discrete sum, $k_m \in \{\frac{2\pi n}{L_m} | n = 0, 1, \dots, L_m - 1\}, 1 \leq m \leq j - 1$. The result, however, remains completely the same as Eq. (S38). In summary, we have

$$\begin{aligned} |\delta \langle \hat{S}(t) \rangle_{L_1 \times \dots \times L_d}| & \leq 4 \sum_{\substack{\alpha_m, \alpha_i, \alpha_j, l \\ 1 \leq p \leq d, a=1, 2 \\ \Delta x_p = \pm(L_p - 1)}} \sqrt{h_{\alpha_i} h_{\alpha_j}} \int_{t_1, 2, 3, 4, k_p} [M_{-k_p}^{3-a} e^{M_{-k_p}(t_4-t_3+t_2-t_1)}]_{\alpha_i \alpha_m} [M_{k_p}^a e^{M_{k_p}(t_2-t_1)}]_{\alpha_j \alpha_m} \\ & \times [e^{M_0 t_1}]_{\alpha_m \alpha_l} \frac{1}{\sqrt{h_{\alpha_m}}} e^{ik_p \Delta x_p} S_l + 4 \sum_{\substack{(i,j) \in \mathcal{S}_p \\ 1 \leq p \leq d}} \int_{t_3, 4} \bar{S}_p^i(t_4) \bar{S}_p^j(t_3)/S, \end{aligned} \quad (\text{S39})$$

where the time integrations are restricted to $0 < t_1 < t_2 < t_3 < t_4 < t$. We now use the same derivation in Eq. (28) of Ref. [78] to upper bound the k integral by its analytic continuation to $i\kappa$. We focus on the first term, since the

second term can be treated in a similar way. We have

$$\begin{aligned}
|\delta\langle\hat{S}(t)\rangle_{L_1\times\dots\times L_d}| &\leq 4 \sum_{\substack{\alpha_m,\alpha_i,\alpha_j,l \\ 1\leq p\leq d,a=1,2}} \sqrt{h_{\alpha_i}h_{\alpha_j}} \int_{t_{1,2,3,4}} \{[M_{i\kappa_p}^{3-a}e^{M_{i\kappa_p}(t_4-t_3+t_2-t_1)}]_{\alpha_m\alpha_i}[M_{i\kappa_p}^a e^{M_{i\kappa_p}(t_2-t_1)}]_{\alpha_j\alpha_m} + (\kappa_p \rightarrow -\kappa_p)\} \\
&\quad \times [e^{M_0t_1}]_{\alpha_m\alpha_l} \frac{1}{\sqrt{h_{\alpha_m}}} e^{-\kappa_p(L_p-1)} S_l + (\text{Term 2}) \tag{S40} \\
&\leq 4 \sum_{\substack{\alpha_i,\alpha_j,l \\ 1\leq p\leq d,a=1,2}} \sqrt{h_{\alpha_i}h_{\alpha_j}} \int_{t_{1,2,3,4}} \{[M_{i\kappa_p}^a e^{M_{i\kappa_p}(t_2-t_1)} DM_{i\kappa_p}^{3-a} e^{M_{i\kappa_p}(t_4-t_3+t_2-t_1)}]_{\alpha_j\alpha_i} + (\kappa_p \rightarrow -\kappa_p)\} \\
&\quad \times \|e^{M_0t_1}\| e^{-\kappa_p(L_p-1)} S_l + (\text{Term 2}) \\
&\leq 8 \sum_{1\leq p\leq d} c_H c_S c_{\kappa_p} \int_{t_{1,2,3,4}} \omega_{i\kappa_p}^3 e^{\omega_{i\kappa_p}(t_4-t_3+2t_2-2t_1)+\omega_0t_1-\kappa_p(L_p-1)} + (\text{Term 2}) \\
&\leq 2 \sum_{1\leq p\leq d} c_H c_S c_{\kappa_p} \frac{e^{2\omega_{i\kappa_p}t-\kappa_p(L-1)}}{2\omega_{i\kappa_p} - \omega_0} + (\text{Term 2}), \tag{S41}
\end{aligned}$$

where $D = \text{diag}\{\frac{1}{\sqrt{h_{\alpha_m}}}\}$, $c_H = \sum_{\alpha_i} h_{\alpha_i}$, $c_S = \sum_{\langle lS \rangle} 2\sqrt{h_l} S$, $c_{\kappa_p} = \|U_{i\kappa_p}\| \|U_{i\kappa_p}^{-1}\| \|U_{i\kappa_p}^{-1} D U_{i\kappa_p}\| + (\kappa_p \rightarrow -\kappa_p)$, $\omega_{i\kappa_p}$ is the Perron-Frobenius eigenvalue of $M_{i\kappa_p}$ (i.e. the eigenvalue with the largest magnitude; this must be real and positive by the Perron-Frobenius theorem), and $U_{i\kappa_p}$ is the matrix that diagonalizes $M_{i\kappa_p}$, i.e. $M_{i\kappa_p} = U_{i\kappa_p} \Omega_{i\kappa_p} U_{i\kappa_p}^{-1}$ for some diagonal matrix $\Omega_{i\kappa_p}$. In the third line we use Cauchy-Schwarz inequality $\sum_{i,j} \sqrt{h_i} C_{ij} \sqrt{h_j} \leq \sum_i h_i \|C\|$. Combined with the second term, the final result is

$$|\delta\langle\hat{S}(t)\rangle_{L_1\times\dots\times L_d}| \leq \sum_{1\leq p\leq d} C_{\kappa_p} e^{2\omega_{i\kappa_p}t-\kappa_p(L-1)}, \tag{S42}$$

where

$$C_{\kappa_p} = 2 \frac{c_H c_S c_{\kappa_p}}{2\omega_{i\kappa_p} - \omega_0} + 8 S c_H \frac{\|U_{i\kappa_p}\|^2 \|U_{i\kappa_p}^{-1}\|^2}{\omega_{i\kappa_p}^2} s_{\kappa_p} s_{-\kappa_p}, \quad s_{\kappa_p} = \sqrt{\sum_{\langle lS \rangle} h_l e^{2\vec{\kappa}_p \cdot (\vec{r}_l - \vec{r}_s)}}. \tag{S43}$$

Notice that $\omega_{i\kappa_p}$ means $\omega_{i\vec{\kappa}_p}$ where the only nonzero component of $\vec{\kappa}_p$ is in the p -th direction equal to κ_p .

With Eq. (S42) we are ready to derive the bound in Eq. (7). The arguments in Sec. IV of Ref. [78] can be generalized to prove the following

Proposition 1. *Let $f(t)$ be a function with Taylor expansion $f(t) = \sum_{n\geq m} f_n t^n$, where m is a positive integer and $f_n \geq 0, \forall n \geq m$. If $f(l/v) \leq C$, then $f(t) \leq C(vt/l)^m$, for $0 \leq t \leq l/v$.*

Now take $f(t) = |\langle\hat{S}(t)\rangle_{c_{p-1}} - \langle\hat{S}(t)\rangle_{c_p}|$. Eq. (S42) proves that $f(\frac{L_p}{2v_p}) \leq C_{\kappa_{p0}} e^{\kappa_{p0}}$ (one has to redo the above derivations for each direction separately), where

$$v_p = \min_{\kappa_p > 0} \frac{\omega_{i\kappa_p}}{\kappa_p} \tag{S44}$$

is the LR speed in the p -th direction, and κ_{p0} is the position of the minimum. On the other hand, using the Taylor expansion of $G_{ij}(t)$ in Eq. (S22), one can show that the upper bound for $f(t)$ given in Eqs. (S30) and (S34) has a Taylor series expansion with the same leading term as the Chen-Lucas bound in Eq. (S11) and with non-negative coefficients, i.e. $f(t) = \sum_{n\geq m} f_n t^n$ where $f_n \geq 0$, and $m = \min n_p(Y_S) - 1$ is the number of Hamiltonian terms of the smallest Y -shape starting from S that is L_p -cell unembeddable in the p -th direction. Therefore, Proposition 1 says

$$|\langle\hat{S}(t)\rangle_{c_0} - \langle\hat{S}(t)\rangle_{c_1}| \leq C_{\kappa_{p0}} e^{\kappa_{p0}} \left(\frac{2v_p t}{L_p}\right)^{\min n_p(Y_S)-1}. \tag{S45}$$

In summary, we have

$$|\delta\langle\hat{S}(t)\rangle_{L_1\times\dots\times L_d}| \leq \sum_{1\leq p\leq d} C_p \left(\frac{2v_p t}{L_p}\right)^{\mathcal{L}_p}, \tag{S46}$$

where $C_p \equiv C_{\kappa_{p0}} e^{\kappa_{p0}}$ and $\mathcal{L}_p \equiv \min n_p(Y_S) - 1$. In general, the exponent \mathcal{L}_p is linearly related to L_p , i.e. $\mathcal{L}_p = \eta_p L_p - \mu_{p,S}$. This finishes the proof of Eq. (7).